Influence of Emissions Normalisation Methods on H_2-CH_4 Fuel Comparisons in Generic and NO_x-Abated Gas Turbine Combustion

Authors:

Tomas Davies [a] – DaviesTL8@cardiff.ac.uk (corresponding author) *Cardiff University*

+44 29 2087 5712

Daniel Pugh [a] – pughdg@cardiff.ac.uk *Cardiff University*

Sally Hewlett [b] – hewletts2@cardiff.ac.uk *Cardiff University*

Steven Morris [b] – morrissm@cardiff.ac.uk *Cardiff University*

Philip Bowen [a] – BowenPJ@cardiff.ac.uk *Cardiff University (Emeritus)*

a) Cardiff School of Engineering, Queen's Buildings, 14-17 The Parade, Cardiff, CF24 3AA, Wales, United Kingdom

b) Gas Turbine Research Centre (Cardiff University), Port Talbot, SA13 2BZ, Wales, United Kingdom

CRediT Authorship Statement

Tomas Davies: Conceptualisation, Methodology, Formal Analysis, Investigation, Data Curation, Writing – Original Draft / Review & Editing, Visualisation

Daniel Pugh: Conceptualisation, Investigation, Resources, Writing – Review & Editing, Supervision

Sally Hewlett: Investigation, Writing – Review & Editing

Steven Morris: Investigation, Project Administration, Writing – Review & Editing

Philip Bowen: Funding Acquisition

Abstract

Parametric experiments were performed using CH_4-H_2 blends to fuel a model gas turbine combustor at elevated inlet conditions, unabated and whilst employing exhaust gas recirculation (EGR) as a NO_x-abatement technique. The purpose was to quantify the performance of conventional dry, 15% O_2 NO_x correction (ISO) against mass by heat input (MBHI) normalisation to experimentally verify simulated work from the literature, while expanding on this work to cover NO_x-abated combustion.

Abbreviations:
H_2 – Hydrogen, CH_4 – Methane, HC – Hydrocarbon, ISO Method – ISO-11042 Normalisation Method, MBHI – Mass By Heat Input, MBWO – Mass By Work Output, GT – Gas Turbine, H_2O – Water, CO_2 – Carbon Dioxide, N2 – Nitrogen, O_2 – Oxygen

NO_x was found to be consistently inflated in H_2 combustion when compared to CH_4 by the ISO method, whereas the MBHI method was found to closely approximate the mass by work output baseline emissions. Multipliers proposed to correct this inflation were shown to be impractical. A fundamental problem in assessing the effectiveness of EGR using the ISO method was identified as it does not account for the additional volumetric dilution introduced, whereas the MBHI normalisation method avoids this issue.

Keywords: Hydrogen, Emissions Normalization, Gas Turbines, NO_x, NO_x-Abatement

Nomenclature

Normalisation Method	Symbol	Definition
Dry, 15% O_2 (ISO)	$EV_{i,dry}$	Dry volumetric exhaust concentration of species, i
	$EV_{i,15,dry}$	Dry, 15% O_2 volumetric exhaust concentration of species, i
	M_{NO_2}	Molar mass of NO_2
	$NOx_{i,15,dry}$	Dry mass by normalised volume basis NO_x (mg/Nm^3)
	$\varphi_{i,wet}$	Volumetric concentration of species, i
	φ_{H_2O}	Volumetric exhaust concentration of H_2O
	$\varphi_{O_2\,dry}$	Dry volumetric exhaust concentration of O_2
Mass By Heat Input MBHI (Theoretical)	Δh_c	Heat of combustion of fuel blend
	$\dot{m}_{NOx}$	Exhaust mass flow of NO_x
	$\dot{Q}_{in}$	Rate of heat input of combustion process
	$\dot{V}_{exhaust}$	Total volumetric exhaust flow
	$\dot{V}_{fuel}$	Volumetric flow of fuel blend
	X_{NOx}	Volumetric exhaust concentration of NO_x
	ρ_{fuel}	Density of fuel blend
	ρ_{NOx}	Density of NO_x
Mass By Heat Input (MBHI - Additional Terms for Practical Considerations)	M_{NO}	Molar mass of NO
	$\dot{m}_{total}$	Total mass flow rate of combustion
	X_{NO}	Volumetric exhaust concentration of NO
	$\sum M_i \cdot X_i$	Summation of the product of the volume fractions and corresponding molar masses of all other species in the exhaust stream
Mass By Work Output (MBWO)	W_{out}	Useful work output of combustion
	η_T	Thermodynamic cycle efficiency

1. Introduction

As hydrogen (H_2) gains prominence for use in gas turbines (GTs), an issue frequently found at the centre of its comparisons to natural gas is NO_x emissions. As a zero-carbon fuel, H_2 is an attractive alternative to hydrocarbon (HC) combustion, however it is well documented that NO_x emissions in H_2 combustion can be significantly higher than those generated by the combustion of natural gas [1–4].

GT emissions reporting is standardised by ISO-11042-1:1996, which specifies acceptable measurement methods, devices and, crucially, normalisation calculations. The standard tool for emissions normalisation in this document is the "dry, 15%$_{vol}$ O_2" method (ISO method), whereby the raw volumetric emissions value has its water (H_2O) fraction removed, and is diluted to a 15% volumetric oxygen (O_2) concentration [5]. Despite this method being an effective tool for comparing HC fuels, Douglas et al. [6] explain the limitations of this method when comparing HC and non-HC fuels and propose an alternative "mass by heat input" technique (MBHI method).

A fundamental difference in the combustion chemistry of H_2 and HCs mean that the ISO emissions reporting method is not an equally representative metric for comparisons of their emissions. In HC combustion, both H_2O and carbon dioxide (CO_2) are produced, with the latter absent from a combusted H_2 product stream. This means that H_2O represents a higher volumetric fraction of the exhaust gases. H_2 combustion also consumes fewer O_2 molecules and thus requires lower relative dilution to reach the target 15% O_2 concentration in the products, at a given operating condition. This serves overall to dilute the NO_x produced from HC fuels more than for the equivalent H_2 flame [6]. Further to this, the removal of the H_2O fraction also exaggerates the appearance of pollutants present in the exhaust stream of H_2 combustion when compared with HC due to this higher concentration of H_2O [6].

Often, strategies for NO_x abatement with H_2 seek to reduce the NO_x produced using dilution to reduce the overall temperature of combustion and therefore reduce thermal NO_x production. Techniques such as exhaust gas recirculation (EGR) or steam injection directly increase the exhaust diluent content and overall volumetric flow, suggesting that, as a volumetric reporting basis, the ISO normalisation method will be further influenced [7–10].

ElKady et al. probed this issue, eventually deriving a hydrocarbon-fuel-specific EGR correction to the ISO normalisation method [11], whilst Weiland et al. derive a relation for the correction for flame diluted with pure N_2 [12], however these remain case-specific solutions. A gap in the literature exists in quantifying how the normalisation technique used influences the observed efficacy of different levels of EGR across varying fuel blends. How this may be augmented by the selection of different normalisation techniques could provide a generalised solution to the problem.

Douglas et al. quantified the difference in emissions figures using fundamental equilibrium stoichiometry for unabated methane-hydrogen (CH_4-H_2) blends [6]. This paper aims to verify their findings and compare the applicability of both the ISO method and MBHI normalisation to experimentally obtained emissions results from a geometrically generic model GT swirl burner, at elevated conditions of inlet temperature and pressure, and determine the influence on the reported NO_x emissions of varying CH_4-H_2 blends.

This paper seeks to expand on the work done by Douglas et al. [6] by applying their methodology to NO_x-abated combustion results. Experiments were performed to quantify the impact of the ISO and MBHI normalisation techniques on the emissions of combustion with EGR, and appraised and quantified across different CH_4-H_2 blends (0-100%$_{vol}$ H_2). EGR was selected to highlight a fundamental problem in using the ISO methodology to report the emissions of diluted combustion, as there is no differentiation between the reduction in NO_x that is genuine (from limiting thermal NO_x production, for example), and that which is simply volumetric dilution. This effect was quantified as part of the work for this paper. In preliminary work, this problem was found to be less pronounced in steam injection (due to ISO emissions reporting mandating the drying of the volumetric water fraction) and closer in line with the results of unabated combustion.

2. Theory

It is significant that any emissions normalisation technique is simply a post-processing step, and therefore has no influence on the actual mass of pollutant emitted in a combustion process. Therefore, it is important to examine any unequal influence defined normalisation processes may have on one fuel over another.

The limitations of conventional normalisation techniques on emissions reporting is beginning to be more widely acknowledged within the combustion sphere, with the UK Department for Environmental, Food and Rural Affairs acknowledging it in recent documentation [13], the European Turbine Network (ETN) and ISO documentation both detailing a series of conversion factors to enable fair, cross-fuel emissions comparison [14,15], and Garan et al. proposing a methodology for deriving conversion factors in their paper [16]. Despite this, conversion factors are not frequently applied in published combustion work. Furthermore, while the practise of simply applying a correction factor to the ISO NO_x figure may initially seem convenient, the technique quickly becomes unwieldy when considering that unique correction factors would be required for individual fuel blends, levels of diluent injection, or different levels of exhaust dilution - for example, the 3% O_2 used as the reference condition for comparing emissions of boilers, as noted by ETN [14].

Emission indices are sometimes used to measure pollutant outputs, and these are generally defined as the mass of pollutant produced per unit mass of fuel consumed, however these indices are of limited use when considering fuels with vastly different caloric content [17].

2.1 Dry, 15% O_2 (ISO) Normalisation

ISO-11042-1:1996 defines two normalisation processes that must be applied to measured emissions [5]. The first is to calculate the dry result, which prevents humidity levels from diluting or exaggerating emissions figures, according to the following equation [5]:

$$EV_{i,dry} = \varphi_{i,wet} \cdot \frac{1}{1-\varphi_{H_2O}} \quad (1)$$

Where $EV_{i,dry}$ (ppm) is the dry volumetric concentration of the exhaust product of interest; $\varphi_{i,wet}$ (ppm) is the measured volumetric concentration of the same product; and φ_{H_2O} is the fractional volumetric concentration of H_2O in the exhaust gas stream.

The second normalisation step in ISO-11042 is to convert to a standardised O_2 level [5]. The standard requires the dry emissions to be normalised to a volumetric O_2 concentration of 15% in accordance with ISO-2533 (to prevent, for example, dilution using excessive exhaust air), using the following equation [5]:

$$EV_{i,15,dry} = EV_{i,dry} \cdot \frac{20.95-15}{20.95-\varphi_{O_2,dry}} \quad (2)$$

Where $EV_{i,15,dry}$ (ppm) represents the volumetric concentration of the exhaust product of interest, dried and diluted to a 15% volumetric O_2 concentration; $\varphi_{O_2,dry}$ (%$_{vol}$) represents the dry volumetric concentration of O_2 in the exhaust gas stream; and $EV_{i,dry}$ (ppm) represents the dry volumetric concentration of the exhaust product of interest.

An amendment to this method, frequently utilised in industry, can be made to normalise NO_x emissions on a dry mass by normalised volume basis ($NOx_{i,15,dry}$ (mg/Nm^3)) according to the following equation:

$$NOx_{i,15,dry} = EV_{i,15,dry} \cdot \frac{M_{NO_2} \cdot 1000}{St.\ Normalised\ Molar\ Volume} \quad (3)$$

In this method, M_{NO_2} (g/mol) represents the molar mass of NO_2, and the volume of standard normalised moles is calculated using the ideal gas equation for reference conditions of 1 atm, 273.15 K. All other symbols are as previously defined.

2.2 Mass by Heat Input (MBHI) Normalisation

The method defined by Equations 1 and 2 (and, by extension, Equation 3) has been the established standard tool for emissions comparisons from HC fuels for many years. Douglas et al. propose alternative normalisation calculations to report figures on a MBHI basis via the following equation [6]:

$$\frac{\dot{m}_{NOx}}{\dot{Q}_{in}} = \frac{X_{NOx} \cdot \rho_{NOx} \cdot \dot{V}_{exhaust}}{\Delta h_c \cdot \rho_{fuel} \cdot \dot{V}_{fuel}} \quad (4)$$

Where X_{NOx} represents the volumetric fraction of the NO_x in the exhaust; ρ (mg/m^3) represents the densities of the pollutant or fuel (as denoted in the subscript of each); Δh_c (MJ/kg) represents the fuel blend heat of combustion; and the $\dot{V}$ (m^3/s) terms represent volumetric flows. Following this convention, $\dot{m}_{NOx}$ (kg/s) is the total mass flow of NO_x in the exhaust, while $\dot{Q}_{in}$ (kW) represents the rate of heat input to combustion [6].

3. Method and Experimental Setup

3.1 Experimental Configuration

Experiments were undertaken utilising the geometrically generic swirl burner at Cardiff University's Gas Turbine Research Centre (GTRC) [18]. The employed system is a modular swirl-stabilised combustor, a typical model for GTs, widely employed in can-annular configurations. The system is housed in an optical pressure casing. The specific geometry and setup are shown in Figures 1 and 2.

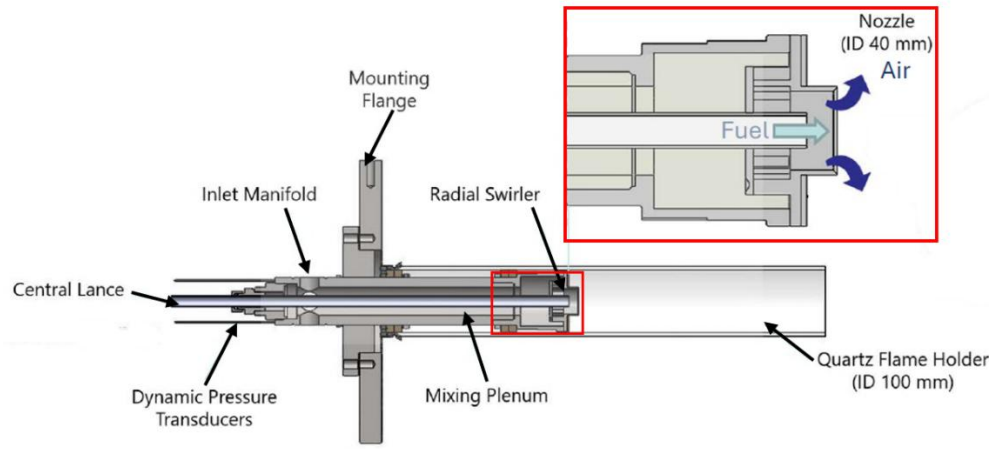

Figure 1: Cross Section of the Combustor Assembly

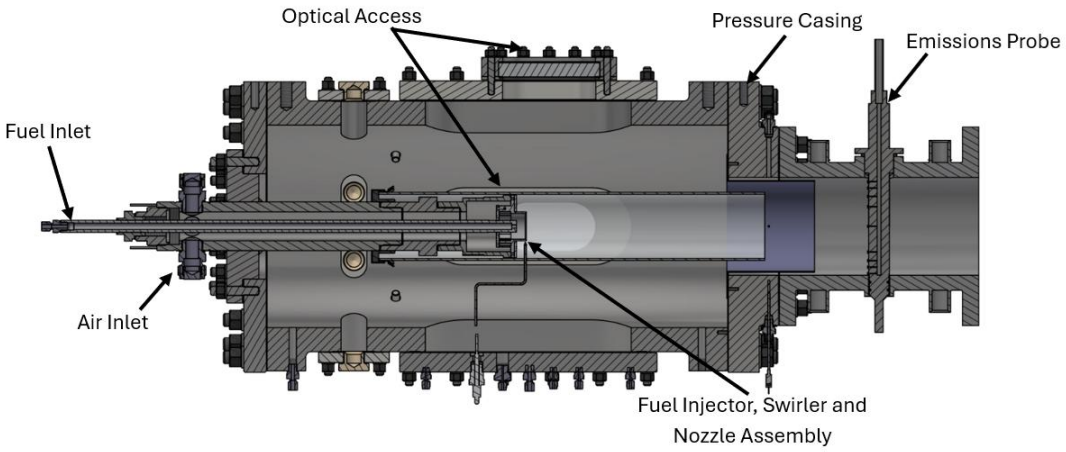

Figure 2: Cross Section of the Combustor Assembled within the High Pressure Optical Casing

The combustor was configured in a non-premixed, co-annular flow configuration. The fuel injector is inserted into the combustion chamber in the form of an 18 mm OD lance which features a 3-hole equilateral plain-orifice fuel injector with a central plain-orifice H_2O injector.

The fuel mixtures in the experiment were blended upstream of the fuel lance. Compressed air entered via the upstream plenum connection, with all flows controlled using a mixture of Coriolis mass-flow controllers (measurement uncertainty ±0.35 – 0.5%) [19,20]. This allowed control of the H_2 volumetric fuel fraction within an absolute uncertainty range of ±1.93%$_{vol}$ at the lowest H_2 condition, decreasing to as low as ±0.38%$_{vol}$ at higher flows, meaning confidence can be taken in the accuracy of the fuel delivery system. Full error analysis and details of the system are available in the supplementary materials. Stoichiometry checks comparing the discrepancy between the theoretical exhaust O_2 from equilibrium simulations and the measured values were carried out for each test condition. The maximum discrepancy across the dataset (calculated as the difference in the simulated volumetric O_2 percentage and the measured volumetric O_2 percentage) was 1.48% (relative), and the mean discrepancy was 0.13%, indicative of good mixing and complete combustion in the flame.

Before data capture, the plenum body was preconditioned to 587 K using preheated air dried to a dew point of 256.15 K (displayed as -17 °C on instrumentation). The system temperatures were allowed at least one hour to stabilise. Air was fed through a radial-tangential swirler, around the central fuel injector, and into the combustion chamber, with a burner exit nozzle radius of 20 mm. The swirler provided a geometric swirl number of approximately 0.8 (with 18 mm OD central lance) and is depicted .

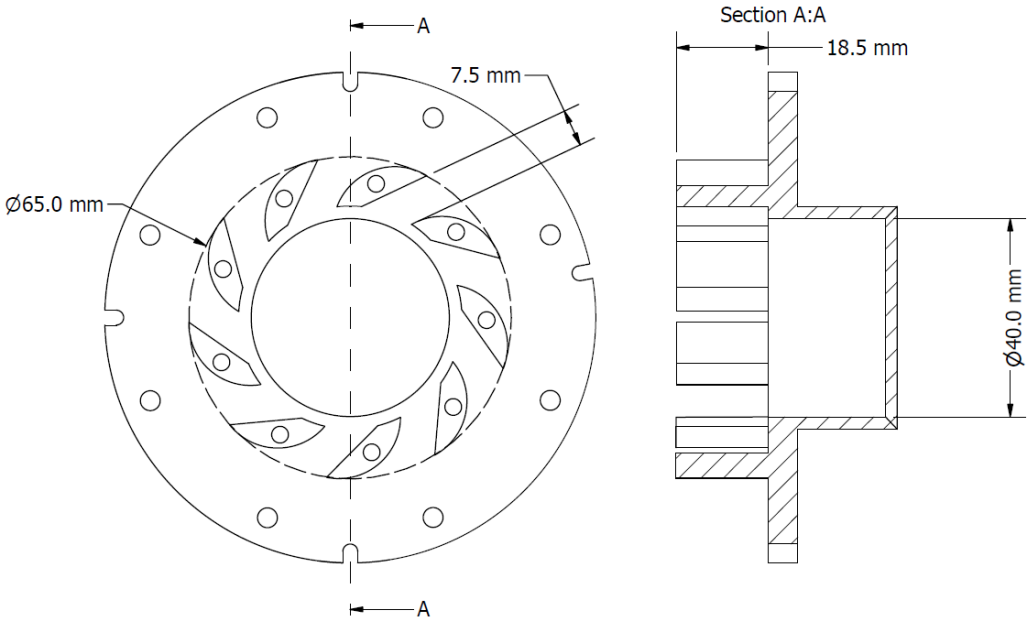

Figure 3: Air Swirler Geometric Details

As shown in Figure 2 previously, the pressure casing features quartz windows, and the flame tube is a 100 mm inner diameter quartz cylinder, allowing optical access. Finally, the system was pressurised according to the condition being targeted, using a water-cooled incremental back-pressure valve downstream of the combustion chamber and a temperature-conditioned emissions probe (at 433 K). A pressure of 0.11 MPa was used to approximate ambient conditions, the slight pressurisation dynamically isolating the rig from the exhaust stack.

3.2 Experimental Diagnostics

Emissions data were captured downstream of the combustor exit and quartz confinement tube using a 9-hole equal-area probe. Using the sampling system set up in accordance with ISO-11042 [5], NO_x concentrations were measured hot and wet at 1 Hz via a Signal 4000VM heated vacuum chemiluminescence analyser. Separate sample gas was cooled using a chiller system to approximately 2°C (reducing molar H_2O concentrations to approximately 0.68% volume), after which CO, CO_2, and O_2 measurements were performed using a Signal 9000MGA that uses nondispersive infrared and paramagnetic analyses techniques. A MATLAB script was used to generate an averaged flame image from video recordings taken using a 12mpx Sony Exmor RS CMOS camera at 60 fps. These were filtered using an image processing software to generate a greyscale image of the flame with much of the visual interference removed. A colormap was applied to the images, for clarity.

3.3 Method and Test Points

The first, unabated stage of the campaign used the range of operating conditions defined in Table 1, and the full experimental matrix is included in the supplemental materials. At each pressure, the thermal power was kept approximately constant and was scaled at a rate of 25 kW per 0.1 MPa allowing a quasi-constant residence time and flow field to be maintained as pressure was increased. The change in fuel composition resulted in a small change in adiabatic flame temperature (AFT) of approximately 0.44%. The airflow for each operating condition was specified to provide an equivalence ratio of approximately 0.6 for the 100% CH_4 experimental points. This airflow was then kept constant as the fuel was transitioned, resulting in an equivalence ratio of approximately 0.5 for the 100% H_2 experimental points. This was to mimic a fuel switching exercise in a practical GT system whereby the air drawn for a specified thermal power would remain approximately constant during the fuel transition. For all power and pressure conditions, an air inlet temperature of 587 K was targeted. The minor variations in air mass flow and inlet temperature are detailed in the supplemental material.

Table 1: Operating Ranges for Unabated NO_x Experiments

Pressure (MPa)	Thermal Power (kW)	Air Flow Rate (g/s)	Fuel Flow Rate (g/s)		Hydrogen Fraction ($\%_{vol}$)
			CH_4	H_2	
0.11	27.5	15.7	0 - 0.55	0 - 0.23	0, 25, 40, 60, 80, 100
0.20	50.0	28.5	0 - 1.00	0 - 0.42	
0.40	100.0	57.1	0 - 2.01	0 - 0.84	
0.60	150.0	85.7	0 - 3.00	0 - 1.25	

In the next stage of the experimental campaign, two fuel blends of 25$\%_{vol}$ H_2 (the remainder being CH_4) and 100% H_2 were used with different levels of synthesised EGR. As the test facility cannot facilitate the actual recirculation of exhaust gases, this was simulated by direct injection of mass flows of air, CO_2, N_2, and H_2O (steam), into the air-fuel mixture from independent gas lines, for both 25$\%_{vol}$ H_2 (75$\%_{vol}$ CH_4) and 100% H_2 cases. The same equivalence ratios and target inlet temperature were used as in the previous stage. The EGR gas flows were delivered in proportion to their mass ratios in the combustion products of the relevant unabated (stage 1) case, modelled under equilibrium conditions, with the remainder of the exhaust gas after accounting for O_2, H_2O and CO_2 modelled as N_2. The mass composition of the injected exhaust gas is detailed in Table 2.

Table 2: EGR Mass Composition

Species	Mass Fraction	
	25%$_{vol}$ H_2 Fuel Blend	100% H_2 Fuel Blend
O_2	0.09	0.11
H_2O	0.08	0.13
CO_2	0.08	0
N_2	0.75	0.76

It is worth noting that, due to the cyclic nature of EGR, using a constant gas composition is not strictly correct. It was verified for a fixed percentage mass recirculated, however, that the composition of the EGR gases approach a point of equilibrium (a percentage change in species fractions of < 0.005%) after 3 iterations of equilibrium simulation. Therefore, a constant EGR composition was considered a suitable surrogate. The system used is perfectly premixed, and as such will not reflect the specificities, mixing characteristics, and timescales of any one industrial EGR system, however this was not the aim of the experimental campaign. Instead, the system represents a generic, lab-scale approximation of an EGR system, and is a standard approach used to assess diluent-based NO_x-abatement [21].

The test points for the level of EGR were 0% (unabated), 8%, 16%, and 24% of the equivalent undiluted exhaust mass flow for the unabated condition, allowing a total EGR mass flow to be defined for each point. The flows of individual gases could then be calculated according to the mass fractions in Table 2. Air was used as one of the EGR gases, and the remainder of the gas required was injected using individual gas flows. Each level of EGR was initially tested with a constant fuel blend of 25%$_{vol}$ H_2 at 27.5 kW$_{th}$ (0.11 MPa), 50 kW$_{th}$ (0.2 MPa) and 100 kW$_{th}$ (0.4 MPa) and then repeated using a 100% H_2 fuel blend. The ranges covered by these test points are summarised in Table 3.

Table 3: Operating Ranges for Exhaust Gas Recirculation Testing

Pressure (MPa)	Thermal Power (kW)	Hydrogen Fraction (%$_{vol}$)	Fuel Flow Rate (g/s)		EGR Fraction (%$_{mass}$)	EGR Flows (g/s)			
			CH_4	H_2		Air	CO_2	H_2O	N_2
0.11	27.5	25	0.5	0.02	0, 8, 16, 24	0 - 1.52	0 - 0.31	0 - 0.31	0 - 1.77
		100	0	0.23		0 - 1.82	0	0 - 0.50	0 - 1.52
0.20	50.0	25	0.91	0.04	0, 8, 16, 24	0 - 2.76	0 - 0.57	0 - 0.57	0 - 3.21
		100	0	0.42		0 - 3.31	0	0 - 0.90	0 - 2.76
0.40	100.0	25	1.82	0.08	0, 8, 16, 24	0 - 5.51	0 - 1.13	0 - 1.13	0 - 6.42
		100	0	0.84		0 - 6.61	0	0 - 1.81	0 - 5.53

3.4 Mass by Heat Input (MBHI) Practical Considerations

Analysing pollutant emissions on a MBHI basis with full accuracy, in practice, requires measurements of the total exhaust volumetric flow rate, as well as the volumetric concentration of exhaust species. Determining the normalised figure is achieved in practice using the following relationship (shown here for NO, but equally applicable to NO_2):

$$NO_{MBHI} = \frac{\dot{m}_{NO}}{\dot{Q}_{in}} = \frac{\dot{m}_{total}}{\dot{Q}_{in}} \cdot X_{NO} \cdot \frac{M_{NO}}{\sum M_i \cdot X_i} \quad (5)$$

Here, $\dot{m}_{total}$ (g/s) represents the total mass flow rate into the system; $\dot{Q}_{in}$ (kW, determined using the known mass flow rates and lower heating values of the fuel) represents the thermal power; X_{NO} represents the volumetric fraction of NO; M_{NO} represents the molar mass of NO (g/mol); and $\sum M_i \cdot X_i$ (g/mol) represents a summation of the product of the volume fractions and corresponding molar masses of all other species in the exhaust stream. It is noteworthy that it was not possible to measure the volume fraction of each species in the exhaust stream. For this experimental campaign, the fractions of O_2, CO_2, NO, and NO_2 were directly measured and used in the calculations. The same equilibrium H_2O fraction that was used for the ISO method (i.e. simulated using Chemkin and the GRI-Mech 3.0 reaction mechanism [22]) was also used in the calculations. The rest of the volume fraction was assumed to be N_2, neglecting argon and trace atmospheric gases.

3.5 Mass by Work Output (MBWO) Normalisation and Cycle Modelling

A MBWO baseline is useful to accurately convey emissions, particularly when considering a fuel switch, which, in practise, would likely occur for a GT employed in an application in which the required work output is fixed. The main difference between the "work output" and "heat input" reporting bases is that the latter does not account for the change in efficiency that results from the changing fuel composition. This can be represented numerically by combining Equations 5 and 6, to form Equation 7:

$$\eta_T = \frac{W_{out}}{Q_{in}} \quad (6)$$

$$NO_{MBWO} = \frac{\dot{m}_{NO}}{\dot{W}_{out}} = \frac{\dot{m}_{total}}{\eta_T \cdot \dot{Q}_{in}} \cdot X_{NO} \cdot \frac{M_{NO}}{\sum M_i \cdot X_i} \quad (7)$$

In these equations, η_T represents the thermodynamic cycle efficiency; W_{out} (kW) represents useful work output; and all other symbols are as defined for equation 5. As before, the equation here is shown for NO, but is also applicable to NO_2.

The experimental apparatus provided no way to determine a cycle work output, therefore, this was simulated using a simple cycle model in Aspen Plus® (Version 12) [23]. The modelling was based on the Peng-Robinson equation of state: a modification of the Van der Waals equation and well suited to modelling non-polar substances [24,25]. Air

was modelled dry, to match the dry air used experimentally, using a volumetric composition of 21% O_2, 78% N_2, and 1% Ar. The model was constructed to simulate the GTRC system. Separate fuel, air and abatement medium streams were connected to an RGibbs reactor. The RGibbs reactor models equilibrium (i.e. complete combustion) by minimising Gibbs free energy: a reasonable assumption given the equivalence ratios of every test point were comfortably lean, ranging from approximately 0.5 – 0.6 across the experimental campaign. The pressures, temperatures and reacting species mass flow rates for the input streams were matched to the measured values at each experimental point. Heat losses within the combustor were neglected, as they were found to have negligible effect on the final relative emissions results.

Finally, to extract a work output, a theoretical turbine was incorporated into the modelling. The turbine was arbitrarily established with 100% mechanical and isentropic efficiencies, discharging at atmospheric pressure. This was justifiable as the aim of this work was to characterise the change in emissions between conditions. Therefore, the important detail to capture for the MBWO metric was the relative *change* in cycle efficiency due to the fuel transition, not specific efficiency values (i.e. by treating the mechanical and isentropic turbine efficiencies as constants, regardless of fuel). The efficiency value for each experimental point was used to determine a work output, and this was combined with the experimentally measured emissions, to determine a MBWO NO_x figure for each experimental condition used as the basis of the comparison central to this work. The assumptions made have, where possible, reflected real test conditions and the theoretical turbine parameters were not modified between points, meaning minimal influence on the final results is to be expected.

3.6 MBWO as a Baseline for NO_x Increases

In their original work [6], Douglas et al. used emissions on a MBWO basis to define a datum NO_x increase between different fuel blends. For ease of comparison, this method was also used in this work. To achieve this, the NO_x at each fuel blend (as a fraction of the NO_x at 100% CH_4) was determined for both the ISO and MBHI cases. These same fractions were then determined on the MBWO basis discussed earlier, which was used as a baseline case for comparison.

This was done by finding a metric termed the “increase ratio”. This represents the fractional NO_x change at a given blend, calculated using either the ISO or MBHI normalisation technique, as a ratio of the same fractional NO_x change on a MBWO basis (effectively showing how closely matched the ISO and MBHI reported NO_x changes, due to a fuel switch, are to the MBWO baseline case. The closer the ratio is to 1, the closer the normalisation technique matches to the MBWO case) [6].

Another advantage of this method as a basis for comparison is that it is relative in nature. This means that any change in conditions that could affect NO_x formation at a

given point (for example, the decision to hold constant airflow across the fuel transition leading to leaner combustion at high H_2 fractions) does not impact the final results. This is because, although the absolute production of NO_x at a given point may be influenced, the metric compares the same change in NO_x between two data points normalised using different techniques. This means any actual changes to raw NO_x emissions will be captured by both normalisation techniques, isolating any discrepancies as a product of the way each normalisation method manipulates the raw figures.

Finally, for clarity, an example of how the increase ratio for the ISO-reported NO_x at 40% H_2 is shown in equation 8.

$$\text{Increase Ratio} = \frac{(\frac{NOx_{40\%H_2}}{NOx_{CH4}})_{ISO}}{(\frac{NOx_{40\%H_2}}{NOx_{CH4}})_{MBWO}} \quad (8)$$

4. Results and Discussion

4.1 Unabated Combustion Emissions Performance

According to the method outlined in section 3, NO_x emissions (representing NO and NO_2) for varying CH_4-H_2 blends, were captured with no abatement. These data, normalised via the ISO method, ISO method converted to a mass per unit normalised volume basis, and MBHI method are shown in Figure 4 (a) and (b).

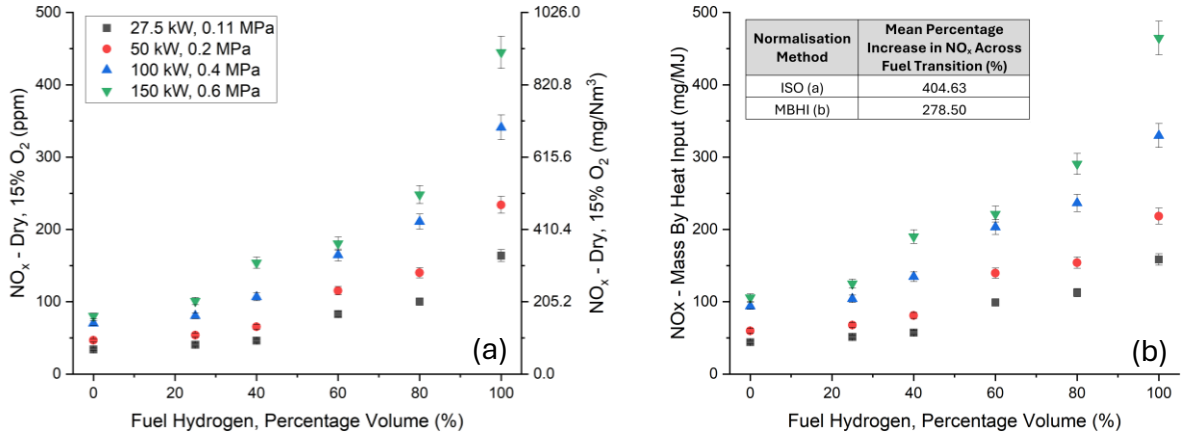

Figure 4: Unabated NO_x Emissions for Varying CH_4-H_2 Fuel Blends at Varying Thermal Power and Pressure Conditions. (a) ISO Normalisation (Left y-Axis) and ISO Normalisation Converted to Mass By Normalised Volume (Right y-Axis); (b) MBHI Normalisation

Clearly, as the H_2 fraction in the fuel increases, so too do the NO_x emissions. This is largely due to increased thermal NO_x production, as described by the Zel'dovich mechanism, which occurs due to higher stoichiometric temperatures and temperature gradients within H_2 flames [26,27]. NO_x production also increases as pressure increases: consistent with established understanding of the N_2O mechanism, which is dominated by third body reactions [27]. At higher H_2 fractions, combustion becomes leaner, moving

away from peak flame speeds [28] and flame temperatures [29], caused by holding a constant air flow as H_2 is introduced. This serves to dampen the NO_x formation associated with increasing H_2 fraction relative to what would be observed were the equivalence ratio held constant, however this will not influence later comparisons of normalisation methods which are conducted relatively.

The two variations of the ISO method in Figure 4 (a) show identical trends, displaying the equivalence between the standard and mass per unit volume versions of the ISO method introduced earlier. As such, these will be considered equivalent and referred to together herein. In contrast to this, while the data in Figure 4 (b) undoubtedly displays a similar trend, there is a significantly lower relative NO_x increase shown across the fuel switch, as quantified in Figure 4.

There are apparent positive inflections in the otherwise relatively smooth curves occurring at 40%$_{vol}$ H_2, in the 150 kW case, and at 60%$_{vol}$ H_2, for the other cases. This inflection is most noticeable in the 150 kW case and reduces in prominence at lower powers and pressures. This inflection is linked with a change in the flame anchoring and global residence time that can be observed optically as the H_2 fraction increases. The changing shape and position of the root of the flame is shown in Figure 5.

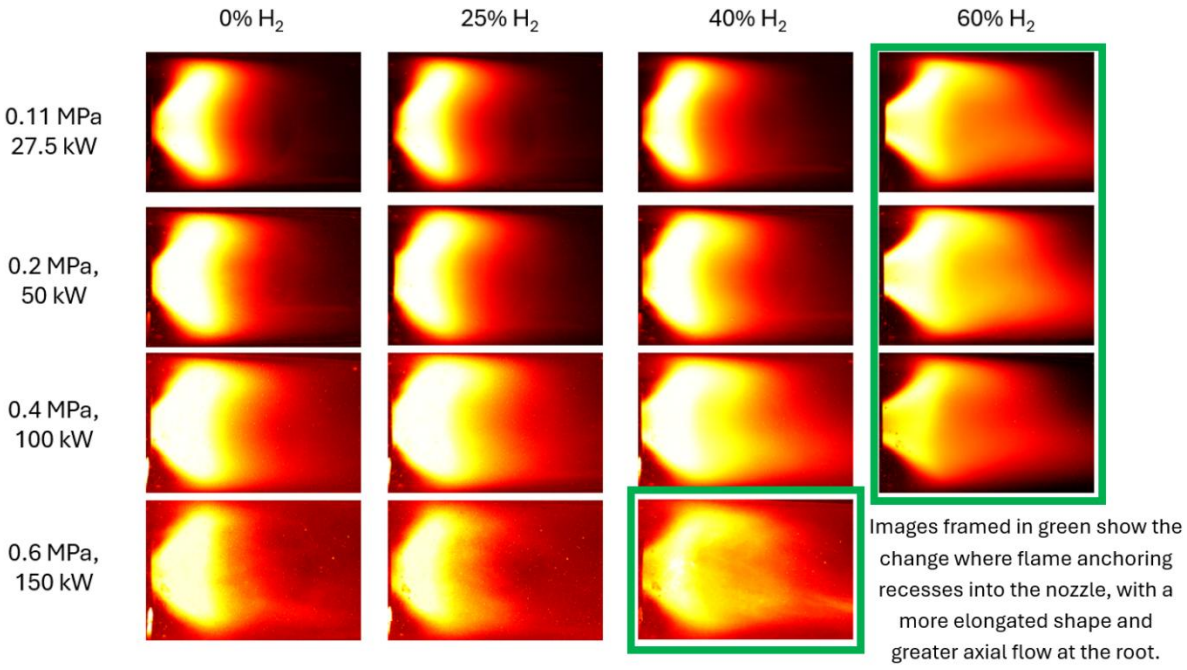

Figure 5: Transition in Flame Anchoring Aligning with Inflections in the NO_x Formation Trends

Between 40 and 60%$_{vol}$ H_2 for the first three cases (27.5 – 100 kW), there is a clear shift to an elongated flame with more axial flow and a more defined edge at the root of the flame due to the increased injection velocity at the higher H_2 blends (due to the decreased density of the mixture, hence increased volumetric flow when maintaining

constant power). The flame also begins recessing into the nozzle as the flame speed and reactivity increase with H_2 addition [30–33].

The change in flame shape occurs at a lower H_2 fraction in the 150 kW case. Shown in Table 4, as the thermal power and pressure increases, there is a negligible change in the AFT of a given CH_4/H_2 blend (less than 0.5%, as simulated by GRI-Mech 3.0 using ANSYS Chemkin).

Table 4: AFTs Simulated Using ANSYS Chemkin for Different Pressures, Thermal Powers, and Fuel Blends

Pressure (MPa)	Thermal Power (kW)	Hydrogen Fraction ($\%_{vol}$)	AFT (K)
0.11	27.5	0.0	1889.91
		100.0	1881.63
0.20	50.0	0.0	1892.51
		100.0	1888.41
0.40	100.0	0.0	1891.67
		100.0	1883.41
0.60	150.0	0.0	1890.37
		100.0	1875.93

Thus, as the thermal power is increased, heat losses stay approximately constant (i.e. a relative decrease), as demonstrated by measured exhaust temperatures increasing with thermal power and pressure. Thus, it can be stipulated that increased combustion temperature increased flame speeds, as shown by Figueroa-Labastida et al. [34], meaning less H_2 addition was required to cause the flame to recess within the nozzle.

Increasing pressure is also known to improve mixing, increasing reactivity and turbulent flame speed, and to reduce flame thickness, increasing the sensitivity of the flame geometry to H_2 addition at high pressures [35,36]. Boushaki et al. [31] showed the burning rate of a given CH_4- H_2 blend increases with increasing pressure.

The steepening of the NO_x emissions curve as the H_2 fraction increases is largely an artefact of the fuel fraction being presented volumetrically. Even at $80\%_{vol}$, due to the almost 8 times lower density (NTP) of H_2 compared with CH_4, H_2 represents less than half of the fuel mass flow [37]. Furthermore, the mass and volumetric energy densities of CH_4 and H_2, mean that on a volumetric basis, for a constant thermal power, even until $60\%_{vol}$ H_2, only around 30% of the calorific value of the fuel blend is provided by H_2, and this rapidly increases at higher H_2 percentage volumes, leading to the steepening curve seen.

The disparity in energy content of the two fuels is lower on a mass basis however. As such, by defining blends using mass fraction, the relationship between NO_x and fuel

H_2 is more linear, with clearer relationships between H_2 addition, NO_x and changes in flame behaviour. This plot is shown in Figure 6.

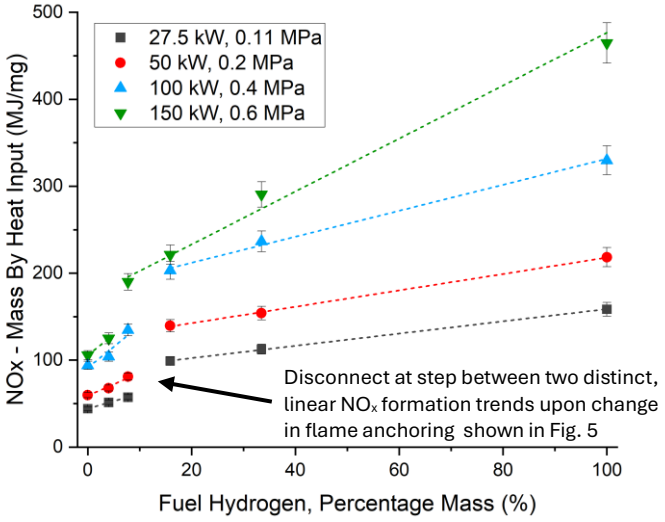

Figure 6: MBHI NO_x Emissions for Varying CH_4-H_2 Fuel Blends, Defined on a Mass Basis, at Varying Thermal Power and Pressure Conditions

There is a near linear NO_x increase when fuel fraction is defined on a mass basis, with the curved relationship of increasing gradient observed volumetrically, now completely absent. Due to the closer spacing of the datapoints at lower H_2 fractions, the inflections previously identified can now be seen as clear step increases in NO_x formation. When plotted this way the "inflections" appear as divides between two distinct, linear NO_x formation regions: one at low H_2 concentrations and one at high H_2 concentrations (hence the two separate trendlines for each dataset). Presenting NO_x emissions on a H_2 $\%_{mass}$ basis serves to more clearly reinforce the concept of the flame anchoring change aligning with increased NO_x occurring at lowering H_2 fractions as pressure and power increase.

4.2 Exhaust Gas Recirculation Emissions Performance

NO_x emissions for varying CH_4-H_2 blends and varying degrees of exhaust gas recirculation were captured. The data at 25%$_{vol}$ and 100% H_2 is plotted in Figure 7. The total EGR mass flow at each test point is defined as a percentage of the total undiluted mass flow, as discussed in section 3.3, with each unit mass of EGR following the mass composition defined previously, in Table 2.

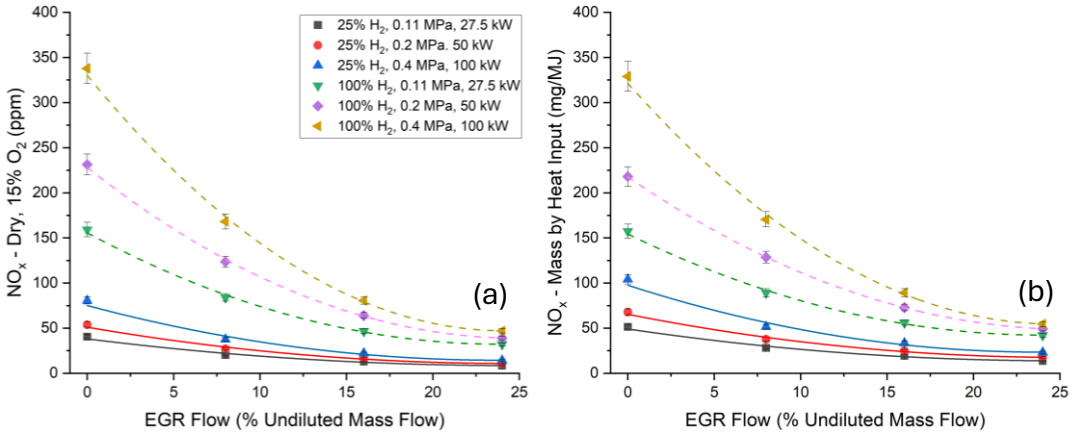

Figure 7: NO_x Emissions for Different Levels of EGR for 25%$_{vol}$ and 100% H_2 Fuel Blends at Varying Thermal Power and Pressure Conditions. (a) ISO Normalisation; (b) MBHI Normalisation

EGR is effective in mitigating NO_x emissions at all pressures, thermal powers, and fuel compositions tested, with a clear reduction in NO_x as the level of EGR is increased. This reduction is achieved by reducing the O_2 concentration and decreasing thermal NO_x production [38]. Data for both normalisation techniques are well characterised by curves of decreasing gradient, with EGR being more effective with increasing H_2 fraction due to its temperature suppression effect and the relative dominance of the thermal mechanism in these flames [39].

Consistently, there appears to be an ultimate minima in NO_x emissions for the 25%$_{vol}$ H_2 cases. All three experiments converge to a similar minimum NO_x at the highest EGR level. The convergence to a minima is also observable in the 100% H_2 experiments. EGR primarily reduces NO_x by inhibiting the thermal formation mechanism, similarly to steam injection (although by reducing the O_2 concentration in the flame compared with acting as a heat-sink [38,40]). Similar convergence to an ultimate maxima in NO_x reduction has been shown theoretically and empirically by Londerville et al. in their paper on steam injection in process burners, implying a maximum potential of thermal-NO_x reduction [41].

Overall, EGR provides a useful means to reduce NO_x in combustion systems – especially in those with H_2-dominated fuel blends – but tends to an ultimate limit in effectiveness.

4.3 Comparison of Emissions Across Normalisation Techniques

4.3.1 Sample Cycle Modelling Output

As an example of the output of the Aspen Plus® simulations performed for every test condition, a sample set of cycle efficiencies (those determined at 0.4 MPa, 100 kW_{th}) are presented in Figure 8. The cycle efficiency can be seen to increase by approximately 0.8% as the fuel transitions from CH_4 to H_2. The full range of simulated efficiencies can be

viewed in the supplementary materials. These were used to calculate a theoretical work output for each experimental condition, allowing the MBWO baseline emissions to be determined.

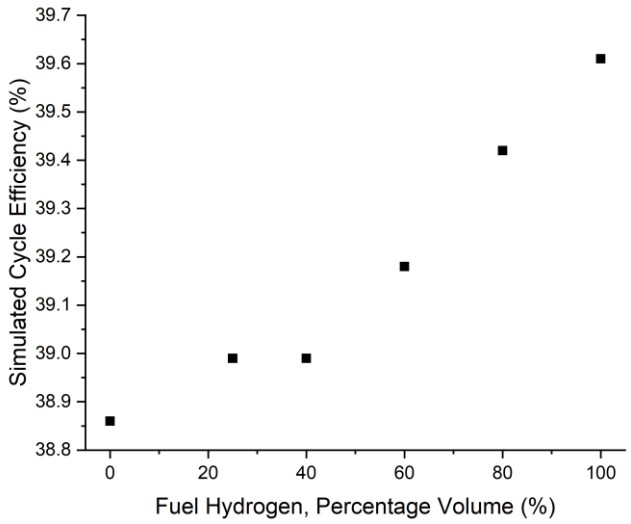

Figure 8: Simulated Cycle Efficiencies for Different CH_4-H_2 Blends at 100 kW_{th} (0.4 MPa)

This increase in efficiency arises due to a slight increase in the product stream volume flow in the pure H_2 combustion (simulated as 0.0836 m^3/s) compared with CH_4 combustion (simulated as 0.0819 m^3/s), meaning more turbine work is done per unit caloric content of the fuel. A greater proportion of work generation as opposed to heat is also indicated by the higher simulated temperature of the product stream for H_2 (1845.81 K) compared with CH_4 (1874.92 K).

4.3.2 Influence of Normalisation Method on Unabated Experiments

The fractional increase in NO_x between 100% CH_4 and 100% H_2 for each operating condition and the ISO and MBHI normalisation techniques is quantified in Table 5. The ISO method consistently exaggerates the NO_x increase when transitioning from CH_4 to H_2, when compared with the MBHI method. The average fractional increases reported by the two methods were 4.05, contrasting with 2.78, respectively, thus ~46% higher on average for the ISO method. However, there is no clear trend in the relative offset between the NO_x increases of the two normalisation methods with changing power, as can be seen characterised by the percentage differences presented.

Table 5: Comparison of ISO and MBHI Normalised NO_x Emissions via Percentage Increases in NO_x Between Pure H_2 and Pure CH_4 Fuel Blends.

Pressure (MPa)	Thermal Power (kW)	Hydrogen Fraction ($\%_{vol}$)	NOx - ISO (ppm)	NOx - MBHI (mg/MJ)	Fractional Increase - ISO	Fractional Increase - MBHI	Percentage Difference in Increases (%)
0.11	27.5	0.0	34.12	44.17	3.8	2.6	46.8
		100.0	163.76	158.46			
0.20	50.0	0.0	46.65	59.88	4.0	2.6	51.7
		100.0	234.00	218.42			
0.40	100.0	0.0	70.18	94.00	3.9	2.5	53.9
		100.0	341.11	329.77			
0.60	150.0	0.0	80.39	105.67	4.5	3.4	33.5
		100.0	444.84	464.63			

The unabated experimental data, are shown using the previously defined "increase ratio" metric in Figure 9. As defined in section 3.7, the bar for each blend represents the averaged increase ratio across the four thermal power and pressure conditions, and an increase ratio of 1 represents a perfect match to the MBWO NO_x increase between 100% CH_4 and the given fuel blend.

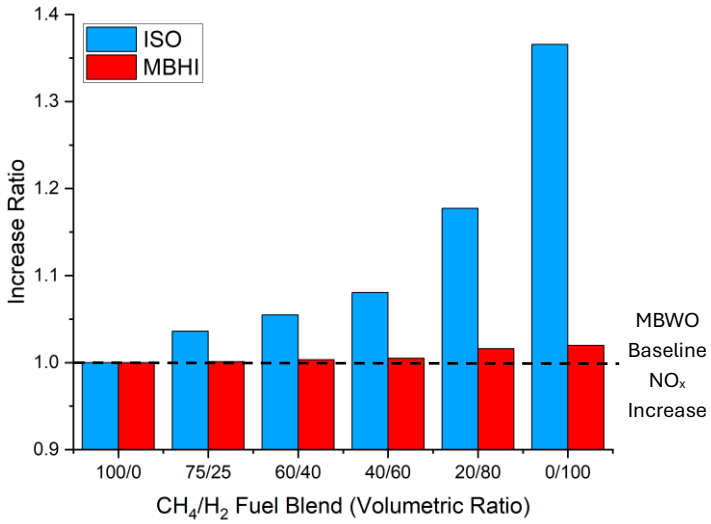

Figure 9: Mean NO_x Increase Ratio at Different Fuel Blends for ISO and MBHI Normalised Emissions. MBWO Baseline at 1.0.

Clearly, the increase in NO_x emissions as the H_2 fraction increases is exaggerated significantly by the ISO normalisation method when compared with MBWO. In contrast to this, normalising on a MBHI basis provides only a minor inflation of around 3% of the MBWO emissions increase, across the fuel switch. The same inflation for the ISO method is around 37%, and this aligns very well with the 36 – 40% figure given by Douglas et al. and shows their simulated results to be reproducible in practice, as well as the 1.372

correction factor proposed by ETN [6,14]. Furthermore, the strong alignment with equilibrium results suggests that incomplete combustion is not influencing the results.

4.3.3 Theoretical Influence of ISO Method on Reported EGR Emissions

EGR achieves NO_x abatement through the injection of some additional volumetric flow, prior to the measurement of emissions [38,40]. Therefore, by definition, NO_x emissions reported on a volumetric basis will be influenced by some pure volumetric dilution as well as a legitimate reduction in NO_x.

To fundamentally assess this influence, simulations were carried out using the open source equilibrium modelling software program Gaseq, which uses the principle of Gibbs free energy minimisation [42]. The reactant mass composition of each EGR abated test point was input into the software. The equilibrium product fractions of H_2O, O_2, NO, NO_2 and CO_2 were recorded (all other product species were assumed as N_2, for simplicity) and were used to assess the effects of volumetric dilution on NO_x emissions normalised using the ISO methodology. To correct for dilution, these exhaust products simply had the mass flows of the additional EGR diluents subtracted, resulting in an exhaust stream free of excess dilution. This approach was made possible by the lean equivalence ratios at which the experiments took place.

This resulted in two exhaust compositions: one uncorrected, and one corrected for excess EGR dilution, and the ISO normalised NO_x was calculated for both. As both the level of dilution caused by the injected exhaust gas and the volumetrically based ISO reporting methodology are intrinsically tied to the species composition of the exhaust stream, the influence of EGR on the results will change on a case-by-case basis. Therefore, determining a universal figure for the relationship between the ISO normalisation method and EGR dilution is not possible, and, as such, the EGR test points used in the practical experiments were targeted. The results are shown in Table 6.

Table 6: Theoretical Influence of EGR Volumetric Dilution on ISO NO_x from Equilibrium Simulation

Fuel Hydrogen Volume Fraction (% Volume)	Equivalence Ratio at 0% EGR	EGR Level (% Undiluted Mass)	Uncorrected		Dilution Corrected		Increase With Dilution Removed (%)
			Dry 15% O_2 NO_x (ppm)	NO_x Fraction (Relative to 0% EGR)	Dry 15% O_2 NO_x (ppm)	NO_x Fraction (Relative to 0% EGR)	
25	0.595	0	940.43	-	940.43	-	-
		8	645.59	0.69	697.76	0.74	8.08
		16	450.96	0.48	523.93	0.56	16.18
		24	316.86	0.34	393.86	0.42	24.30
100	0.501	0	1248.47	-	1248.47	-	-
		8	849.04	0.68	921.16	0.74	8.49
		16	582.76	0.47	681.88	0.55	17.01
		24	404.20	0.32	507.46	0.41	25.55

As can be observed, the figure corrected for pure volumetric dilution shows a lower reduction in NO_x relative to the unabated point, compared to the uncorrected figures. When comparing the NO_x fractions reported by the two methods, removing the dilution of the EGR can be seen to result in up to 25.55% higher NO_x. The discrepancy between the corrected and uncorrected NO_x increases with the level of EGR as the effectiveness reduces, and dilution makes up an increasing portion of the plateauing NO_x reduction. The dilution makes up a slightly higher portion of the NO_x reduction in the pure H_2 flame due to the different composition of the exhaust gases in the two flames. For the pure H_2 flame, each percentage mass of EGR injected represents a higher volumetric flow, meaning a greater volumetric flow is also removed to account for dilution. For a given EGR level, the increase in NO_x seen by removing dilution is 5.1% higher in the 100% H_2 flame than the 25%$_{vol}$ H_2.

Through its drying step, the ISO methodology accounts for any additional H_2O injected, however the remaining EGR gases will cause a reduction in the apparent NO_x concentration through pure volumetric dilution. The second stage of the ISO reporting method requires a dilution to 15%$_{vol}$ O_2, and this stage significantly reduces the influence of dilution by O_2. To quantify this influence, the change in NO_x resulting from the 15% O_2 dilution stage, for both the corrected and uncorrected NO_x emissions, is quantified as a fraction in Table 7.

Table 7: Influence of 15% O_2 Dilution on Raw EGR Emissions and EGR Emissions Corrected for Excess Dilution from Equilibrium Simulation

Fuel Hydrogen Volume Fraction (% Volume)	EGR Level (% Undiluted Mass)	Fraction of Dry 15% O_2 NO_x Relative to Dry NO_x		Difference (%)
		Uncorrected	Corrected	
25	0%	0.497	0.497	0.00
	8%	0.498	0.499	0.04
	16%	0.499	0.499	0.09
	24%	0.499	0.500	0.15
100	0%	0.635	0.635	0.00
	8%	0.635	0.637	0.29
	16%	0.635	0.639	0.58
	24%	0.634	0.640	0.85

Due to the composition of the EGR and the relatively (to the other EGR gases) high molar weight of O_2, O_2 represents a lower volumetric portion of EGR, per unit mass. This means correcting for (i.e. removing) the EGR gas actually serves to inflate the mole fraction of O_2 in the exhaust stream, explaining why NO_x is higher following the 15% O_2 dilution, after correction. This effect increases as the level of EGR increases.

Clearly, there is also a changing effect dependant on the fuel composition. The 15% O_2 dilution reduces the NO_x of the 100% H_2 fuel significantly less, due to its lower O_2

consumption, as already discussed. This also leads to the higher percentage difference between the corrected and uncorrected fraction for the 100% H_2 fuel. The discussed increase in the exhaust O_2 mole fraction, after correcting for the excess EGR gas is exaggerated for the 100% H_2 case.

Despite this, the percentage difference seen over the 15% O_2 dilution stage is 0.85% at a maximum, when correcting for EGR dilution: a small contribution compared to the up to 25.55% difference in overall ISO NO_x shown earlier. This demonstrates that the problems with reporting EGR-abated NO_x emissions using the ISO method are, in the main, caused by dilution from the other (non-H_2O and O_2) recirculated gases that are unaccounted for in the normalisation methodology, and that the influence of the 15% O_2 dilution is far more strongly linked with fuel composition, than dilution.

Overall, volumetric dilution is shown to account for a significant portion (up to 25.55%) of the ISO-reported NO_x reduction in EGR-abated combustion. The proportion of the reduction caused by volumetric dilution increases as the level of EGR increases, and this effect is consistently more significant in high H_2 flames (per unit mass recirculation) due to the higher volume of their recirculated products. The drying stage of the ISO methodology accounts for any H_2O dilution, and the influence of the 15% O_2 dilution between corrected and uncorrected results was shown to be minimal (although the bias against high H_2 fuel still remained), indicating that excess gases that are unaccounted for in the ISO normalisation methodology drive misleading NO_x emissions figures.

4.3.4 Influence of Normalisation on EGR Experiments

The quantitative fractional change in NO_x for EGR, for 25%$_{vol}$ and 100% H_2, averaged across all thermal power and pressure experiments, and relative to the unabated emissions of each fuel composition, is displayed in Figure 10.

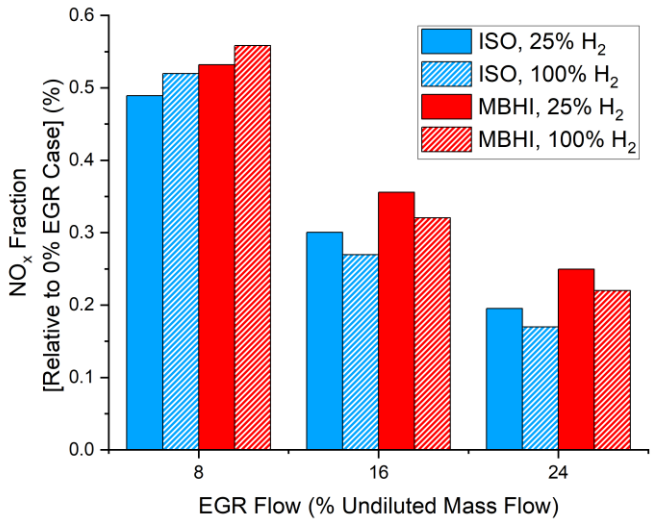

Figure 10: NO_x Fraction (NO_x at given degree of EGR as a fraction of the NO_x with no EGR) for Different Levels of EGR

Quantitively, the apparent efficacy of EGR is reduced when normalised on a MBHI basis compared with the ISO method. EGR is shown to be more effective in the pure H_2 flame at 16% and 24% EGR, but more effective in the 25%$_{vol}$ H_2 fame at 8% EGR, and this trend is consistent across results normalised by both methods.

The data shows the average fractional NO_x at each degree of EGR being consistently higher when normalising on a MBHI basis, compared with the ISO method. The fractional NO_x shown using the ISO method represents, on average, 87% of the fractional NO_x of the MBHI method. This ranges from a maximum of approximately 93% at 8% EGR, to a minimum of approximately 77% at 24% EGR. This suggests a reduction in the apparent efficacy of EGR as a NO_x abatement technique when applying the MBHI normalisation method, with the disparity increasing with increasing EGR.

Earlier, an estimation was made of the degree to which pure volumetric dilution was responsible for the NO_x reduction by EGR when normalising results using the ISO method. At each level of EGR, the discrepancy in the NO_x fraction between the corrected and uncorrected equilibrium ISO results align well with the discrepancy between the practical ISO and MBHI results seen in Figure 10. This suggests that the divergence in NO_x fraction seen in practise between the ISO and MBHI results is a result of volumetric dilution, and further suggests the MBHI metric as more robust in assessing the efficacy of diluent-based NO_x abatement. This is quantified in the supplemental materials.

The influence of changing fuel composition on the emissions, reported by the two normalisation techniques when using EGR, is quantified in Table 8.

Table 8: Comparison of ISO and MBHI Normalised NO_x Emissions via Percentage Increases in NO_x Between Pure H_2 and 75/25 CH_4/H_2 Fuel Blends (on a volumetric basis), with Different Levels of EGR.

Pressure (MPa)	Thermal Power (kW)	EGR Mass Fraction (%)	Fractional Increase in NO_x at 100%$_{vol}$ H_2 from 25%$_{vol}$ H_2		Percentage Difference in Increases (%)
			ISO	MBHI	
0.11	27.5	0.0	2.93	2.06	41.9
		8.0	3.15	2.18	44.4
		16.0	2.60	1.89	37.5
		24.0	2.80	2.06	35.4
0.20	50.0	0.0	3.30	2.21	49.1
		8.0	3.57	2.42	47.8
		16.0	2.89	1.92	50.8
		24.0	2.63	1.81	44.8
0.40	100.0	0.0	3.19	2.16	47.5
		8.0	3.48	2.31	50.5
		16.0	2.63	1.66	58.4
		24.0	2.28	1.36	68.2

As with the steam injection, the NO_x increase shown via the ISO method is significantly higher, on average 48.6% higher, than for MBHI. At 100kW, the offset between the two normalisation techniques increases. This aligns with the theoretical expectation: driven by the increased volumetric dilution in the H_2 flame, as discussed earlier. Despite this, this is not consistently observed across the two lower thermal power cases, for which the trends are considerably more noisy. The trend of the offset increasing with EGR is present when averaging across all thermal power conditions, but the variance across some of the points devalues the mean percentage differences.

For EGR, the NO_x increase reported by the two normalisation techniques has again been determined. This is shown, averaged across all thermal power and pressure cases, between 25%$_{vol}$ H_2 and 100% H_2 in Figure 11.

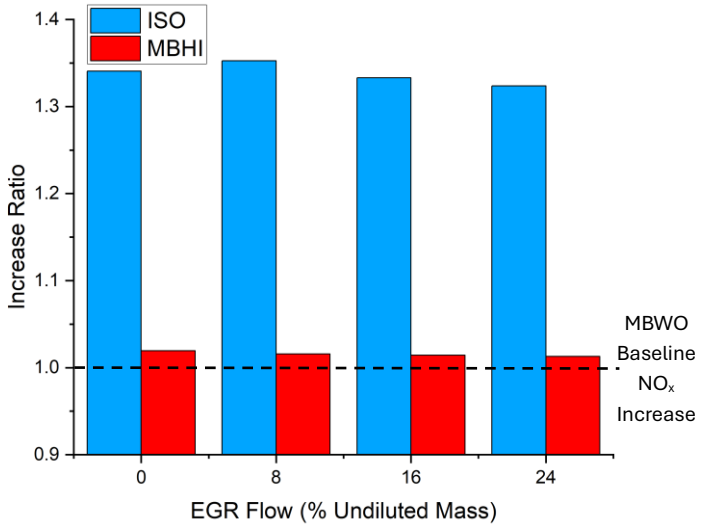

Figure 11: Mean NO_x Increase Ratio (Relative to 25%$_{vol}$ H_2 Respective Cases) at Different Levels of EGR as a Fraction of NO_x at 100% CH_4 for ISO and MBHI Normalised Emissions. MBWO Baseline at 1.0.

Again, the NO_x increase was shown to be inflated by the ISO method. In this case, a difference in the increase reported was up to around 35% greater than the MBWO baseline. The MBHI method provided a closer approximation to MBWO, with an increase ratio at around 2% greater than the MBWO baseline, at a maximum.

4.3.5 Equilibrium Comparisons and Summary of Normalisation Influence

As previously discussed, the results of the unabated experiments matched well with the equilibrium simulations conducted by Douglas et al. [6]. To assess this for the EGR experiments, the results of the previously discussed equilibrium simulations (section 4.3.3) carried out using the Gaseq software were used [42]. Using the simulated exhaust product fractions, NO_x emissions were determined using the ISO, MBHI, and MBWO methods, and were compared relatively using the previously defined “increase ratio”.

The slow chemical kinetics of NO_x formation in nitrogen-free fuels mean that equilibrium modelling consistently overestimates the NO_x generated by a flame, due to the assumption of infinite residence time, to allow all species to reach a point of chemical equilibrium [43,44]. In NO_x abated flames, the final products are even further from this equilibrium point, meaning much higher NO_x figures are simulated than found in practise. Despite this, the use of the increase ratio allows a relative comparison over the fuel switch for the different levels of abatement, irrespective of the discrepancies between the raw and simulated NO_x figures.

An average increase ratio using MBWO as the basis was determined for each level of EGR (across the different levels of thermal power and pressure tested), and these are tabulated in Table 9 along with their experimentally derived counterparts.

Table 9: Comparison of Increase Ratios (MBWO basis) Determined Experimentally and Using Equilibrium Simulations for NO_x-Abated Experiments

EGR Flow (% Undiluted Mass)	Increase Ratio - MBWO Baseline = 1.00			
	ISO		MBHI	
	Experimental	Equilibrium	Experimental	Equilibrium
0	1.34	1.34	1.02	1.02
8	1.35	1.34	1.02	1.02
16	1.33	1.34	1.01	1.02
24	1.32	1.34	1.01	1.01

The experimental and equilibrium increase ratios compare relatively well. The MBHI increase ratios derived from equilibrium simulation are well matched to those derived experimentally, with no difference to two decimal places. This is because the discrepancy between the MBHI normalisation method differs from the MBWO baseline only by the inclusion of cycle efficiency and therefore the MBHI increase ratio is independent of the actual composition of the exhaust stream. Because of expected discrepancies between the experimental and simulated exhaust stream compositions, the experimental and simulated increase ratios for the ISO methodology match less closely, but are broadly representative of one another.

As discussed at the beginning of this paper, one of the proposed solutions to better tailor the ISO normalisation method to HC-H_2 fuel emissions comparisons is to implement correction multipliers to final emissions figures [14,15]. While this is feasible for simplistic comparisons of, for example, CH_4 versus H_2, this paper has demonstrated that the influence of the ISO method on NO_x emissions is non-constant, changing with intermediate blends of fuels and changes to exhaust composition due to NO_x-abatement and dilution. The multiplier approach would require a unique correction factor for each possible combination of fuel composition, and level of NO_x-abatement and dilution – an extremely unwieldy approach compared with a more robust alternative emissions normalisation method such as the MBHI approach discussed in this paper.

5. Conclusions

- In the non-premixed, co-annular flow burner, NO_x production increases with H_2 fraction. When characterised against H_2 volume fraction, NO_x is produced at a non-linear, increasing rate with increasing fuel H_2. When characterised against H_2 mass fraction, NO_x increases more linearly however, highlighting the steepening rate of NO_x production as an artefact of defining gaseous fuel blends on a volumetric basis for fuels of radically different volumetric energy density (e.g. CH_4 and H_2). As fuel H_2 increased, two distinct NO_x formation trends (due to a change in flame anchoring) were identified by defining fuel blends on a mass basis.
- For the unabated experimental work, the ISO-11042 method normalised NO_x increase, for a full CH_4 to H_2 fuel switch, was approximately 37% greater than the MBWO baseline (i.e. increase ratio of 37%). This aligns with the 36 – 40% figure provided by Douglas et al [6].
- For the EGR experiments, the ISO method increase ratio ranged between 32 – 35%, decreasing as the level of EGR increased due to increasing volumetric dilution. These increase ratios matched closely to those determined theoretically using equilibrium modelling.
- The constantly changing effect of combustion conditions (fuel composition, excess dilution) on the extent of distortion of ISO-normalised NO_x figures was demonstrated, showing the potential unwieldiness of proposed correction multipliers. For EGR, additional distortion (to the established fuel bias) was shown to be driven by any non-O_2/H_2O dilution introduced. This issue did not impact the MBHI-reported emissions data.
- The alternative MBHI metric performed well, representing, at a maximum a 2% overestimation of the MBWO NO_x increase when transitioning from CH_4 to H_2 (i.e. increase ratio), including with NO_x abatement, applicable to modelled cycle efficiencies. There was negligible change in the MBHI increase ratio for all experimental conditions, suggesting it to be more robust than the ISO method, and a universal alternative to case-specific modification formulae, or fuel-dependent correction factors.
- A fundamental overestimation of the reduction in NO_x by the ISO method when introducing EGR was found theoretically, using equilibrium modelling. This was due to the ISO method not accounting for the additional volumetric dilution and changed with the level of EGR. The discrepancy between the practical ISO and MBHI NO_x emissions matched well to the theoretical discrepancy determined, suggesting that the MBHI method is more suitable for assessing EGR NO_x.

6. Acknowledgements

I would like to express massive thanks to Dr Daniel Pugh and Dr Sally Hewlett who have provided me with invaluable guidance and feedback when producing this paper, and to Steven Morris for proof-reading the final draft. I would like to express gratitude to Steven Morris, Dr Burak Goktepe and Dr Sally Hewlett, for the data gathering for this paper, and to Prof Philip Bowen who was responsible for the funding acquisition.

Any supplementary data for this study can be accessed through the following repository: [https://doi.org/10.17035/cardiff.30517955].

Funding: This project has been funded by National Gas Transmission Plc and conducted in collaboration with Cardiff University via the Network Innovation Allowance (NIA) funding mechanism from Ofgem, to build knowledge and facilitate the energy transition for gas consumers and end-users.

References

[1] Douglas C, Emerson B, Lieuwen T, et al. NOx Emissions from Hydrogen-Methane Fuel Blends. 2022.

[2] İlbas M, Yılmaz İ, Kaplan Y. Investigations of hydrogen and hydrogen–hydrocarbon composite fuel combustion and NOx emission characteristics in a model combustor. Int J Hydrog Energy 2005;30:1139–47. https://doi.org/10.1016/j.ijhydene.2004.10.016.

[3] Cellek MS, Pınarbaşı A. Investigations on performance and emission characteristics of an industrial low swirl burner while burning natural gas, methane, hydrogen-enriched natural gas and hydrogen as fuels. Int J Hydrog Energy 2018;43:1194–207. https://doi.org/10.1016/j.ijhydene.2017.05.107.

[4] Alhuyi Nazari M, Fahim Alavi M, Salem M, et al. Utilization of hydrogen in gas turbines: a comprehensive review. Int J Low-Carbon Technol 2022;17:513–9. https://doi.org/10.1093/ijlct/ctac025.

[5] British Standards Institution. BS ISO 11042-1:1996 Gas turbines - Exhaust gas emission - Part 1: Measurement and evaluation 1996.

[6] Douglas CM, Shaw SL, Martz TD, et al. Pollutant Emissions Reporting and Performance Considerations for Hydrogen–Hydrocarbon Fuels in Gas Turbines. J Eng Gas Turbines Power 2022;144. https://doi.org/10.1115/1.4054949.

[7] Sehat A, Ommi F, Saboohi Z. Effects of steam addition and/or injection on the combustion characteristics: A review. Therm Sci 2021;25:1625–52. https://doi.org/10.2298/tsci191030452s.

[8] Li H, ElKady A, Evulet A. Effect of Exhaust Gas Recirculation on NOx Formation in Premixed Combustion System. Sess. PC-1 Adv. Combust. Technol., Orlando, Florida: American Institute of Aeronautics and Astronautics; 2009. https://doi.org/10.2514/6.2009-226.

[9] Ditaranto M, Li H, Løvås T. Concept of hydrogen fired gas turbine cycle with exhaust gas recirculation: Assessment of combustion and emissions performance. Int J Greenh Gas Control 2015;37:377–83. https://doi.org/10.1016/j.ijggc.2015.04.004.

[10] Sebastian Göke, Christian Oliver Paschereit. Influence of Steam Dilution on Nitrogen Oxide Formation in Premixed Methane/Hydrogen Flames. J Propuls Power 2011;29:249–60. https://doi.org/10.2514/1.B34577.
[11] ElKady AM, Evulet A, Brand A, et al. Exhaust Gas Recirculation in DLN F-Class Gas Turbines for Post-Combustion CO2 Capture, American Society of Mechanical Engineers Digital Collection; 2009, p. 847–54. https://doi.org/10.1115/GT2008-51152.
[12] Weiland N, Chen R-H, Strakey P. Effects of coaxial air on nitrogen-diluted hydrogen jet diffusion flame length and NO*x* emission. Proc Combust Inst 2011;33:2983–9. https://doi.org/10.1016/j.proci.2010.06.075.
[13] Lewis AC, Allan J, Barnes J, et al. Air pollution arising from hydrogen combustion. Department for Environment, Food and Rural Affairs; 2023. https://doi.org/10.5281/ZENODO.8158664.
[14] ETN. Proposed NOx emissions reporting for hydrogen-containing fuels. 2023.
[15] British Standards Institution. BS EN ISO 16911-1:2013 Stationary source emissions. Manual and automatic determination of velocity and volume flow rate in ducts. Part 1: Manual reference method 2013.
[16] Garan N, Dybe S, Paschereit CO, et al. Consistent emission correction factors applicable to novel energy carriers and conversion concepts. Fuel 2023;341:127658. https://doi.org/10.1016/j.fuel.2023.127658.
[17] 14.3. Emission Indices n.d. https://ansyshelp.ansys.com/public//Views/Secured/corp/v242/en/chemkin_th/pgfId-1125117.html?q=emission%20indices (accessed October 7, 2025).
[18] Pugh D, Runyon J, Bowen P, et al. An investigation of ammonia primary flame combustor concepts for emissions reduction with OH*, NH2* and NH* chemiluminescence at elevated conditions. Proc Combust Inst 2021;38:6451–9. https://doi.org/10.1016/j.proci.2020.06.310.
[19] Coriolis mass flow meters and controllers for liquids and gases. Bronkhorst n.d. https://www.bronkhorst.com/products/liquid-flow/mini-cori-flow/ (accessed February 7, 2026).
[20] Micro Motion ELITE CMF010M Coriolis Meter, 1/10 Inch (DN2), 316L Stainless Steel | EMR n.d. https://www.emerson.com/en-gb/catalog/micro-motion-sku-cmf010m-en-gb?fetchFacets=true#facet:&partsFacet:&modelsFacet:&facetLimit:&searchTerm:&partsSearchTerm:&modelsSearchTerm:&productBeginIndex:0&partsBeginIndex:0&modelsBeginIndex:0&orderBy:&partsOrderBy:&modelsOrderBy:&pageView:list&minPrice:&maxPrice:&pageSize:&facetRange:& (accessed February 7, 2026).
[21] R Marsh, A Giles, J Runyon, et al. SELECTIVE EXHAUST GAS RECYCLING FOR CARBON CAPTURE APPLICATIONS: COMBUSTION AND OPERABILITY MEASUREMENT, Brussels, Belgium: ETN Global; 2016.
[22] Michael Frenklach, Tom Bowman, Greg Smith. GRI-Mech Home Page n.d. http://combustion.berkeley.edu/gri-mech/ (accessed April 28, 2025).
[23] Aspen Plus | Leading Process Simulation Software | AspenTech n.d. https://www.aspentech.com/en/products/engineering/aspen-plus (accessed July 31, 2025).
[24] Peng D-Y, Robinson DB. A New Two-Constant Equation of State. Ind Eng Chem Fundam 1976;15:59–64. https://doi.org/10.1021/i160057a011.

[25] J. F. Boston, P. M. Mathias. Phase Equilibria in a Third-Generation Process Simulator, Berlin: Department of Chemical Engineering and Energy Laboratory, Massachusetts Institute of Technology; 1980, p. 823–49.
[26] Yakov Borisovich Zel'dovich. The Oxidation of Nitrogen in Combustion Explosions. Acta Physiochemica 1946;21:577–628.
[27] Cecere D, Giacomazzi E, Di Nardo A, et al. Gas Turbine Combustion Technologies for Hydrogen Blends. Energies 2023;16:6829. https://doi.org/10.3390/en16196829.
[28] He X, Hou X, Yang Q, et al. Study of laminar combustion characteristics of gasoline surrogate fuel-hydrogen-air premixed flames. Int J Hydrog Energy 2019;44. https://doi.org/10.1016/j.ijhydene.2019.03.009.
[29] Ciniviz M, Köse H. HYDROGEN USE IN INTERNAL COMBUSTION ENGINE: A REVIEW n.d.
[30] Li Z, Cheng X, Wei W, et al. Effects of hydrogen addition on laminar flame speeds of methane, ethane and propane: Experimental and numerical analysis. Int J Hydrog Energy 2017;42:24055–66. https://doi.org/10.1016/j.ijhydene.2017.07.190.
[31] Boushaki T, Dhué Y, Selle L, et al. Effects of hydrogen and steam addition on laminar burning velocity of methane–air premixed flame: Experimental and numerical analysis. Int J Hydrog Energy 2012;37:9412–22. https://doi.org/10.1016/j.ijhydene.2012.03.037.
[32] Cheng X, Scribano G. Effects of hydrogen addition on the laminar premixed flames and emissions of methane and propane. Int J Hydrog Energy 2024;53:1–16. https://doi.org/10.1016/j.ijhydene.2023.12.040.
[33] Chen Z. Effects of hydrogen addition on the propagation of spherical methane/air flames: A computational study. Int J Hydrog Energy 2009;34:6558–67. https://doi.org/10.1016/j.ijhydene.2009.06.001.
[34] Figueroa-Labastida M, Zheng L, Streicher JW, et al. Effect of elevated temperatures (550–860 K) on the laminar flame speeds of methane/hydrogen blends. Fuel 2024;372:132219. https://doi.org/10.1016/j.fuel.2024.132219.
[35] Rieth M, Gruber A, Chen JH. The effect of pressure on lean premixed hydrogen-air flames. Combust Flame 2023;250:112514. https://doi.org/10.1016/j.combustflame.2022.112514.
[36] Saccone G, Marini M. Chemical Kinetic Analysis of High-Pressure Hydrogen Ignition and Combustion toward Green Aviation. Aerospace 2024;11:112. https://doi.org/10.3390/aerospace11020112.
[37] Klebanoff LE, Pratt JW, LaFleur CB. Comparison of the safety-related physical and combustion properties of liquid hydrogen and liquid natural gas in the context of the SF-BREEZE high-speed fuel-cell ferry. Int J Hydrog Energy 2017;42:757–74. https://doi.org/10.1016/j.ijhydene.2016.11.024.
[38] Wei H, Zhu T, Shu G, et al. Gasoline engine exhaust gas recirculation – A review. Appl Energy 2012;99:534–44. https://doi.org/10.1016/j.apenergy.2012.05.011.
[39] Cecere D, Carpenella S, Giacomazzi E, et al. Effects of hydrogen blending and exhaust gas recirculation on NOx emissions in laminar and turbulent CH4/Air flames at 25 bar. Int J Hydrog Energy 2024;49:1205–22. https://doi.org/10.1016/j.ijhydene.2023.10.172.
[40] Zhao D, Yamashita H, Kitagawa K, et al. Behavior and effect on NOx formation of OH radical in methane-air diffusion flame with steam addition. Combust Flame 2002;130:352–60. https://doi.org/10.1016/S0010-2180(02)00385-1.

[41] Londerville S, Anderson K, Baukal C, et al. Water/Steam Injection for NOx Reduction in Process Burners, American Society of Mechanical Engineers Digital Collection; 2019. https://doi.org/10.1115/IMECE2018-88688.
[42] Chris Morley. Gaseq Chemical Equilibrium Program n.d. http://www.gaseq.co.uk/ (accessed August 29, 2025).
[43] Mazzotta L, Meloni R, Lamioni R, et al. Numerical Investigation of NOx emissions in a gas turbine burner using hydrogen-ammonia and partially cracked ammonia fuel blends: A combined LES and CRN approach. Appl Therm Eng 2025;278:127330. https://doi.org/10.1016/j.applthermaleng.2025.127330.
[44] Eggersmann M, Hackenberg J, Marquardt W, et al. Chapter 5.1 - Applications of Modelling – A Case Study from Process Design. In: Braunschweig B, Gani R, editors. Comput. Aided Chem. Eng., vol. 11, Elsevier; 2002, p. 335–72. https://doi.org/10.1016/S1570-7946(02)80017-7.